

# Nanoparticle analysis using microscale field flow fractionation

Bruce K. Gale\* and Himanshu J. Sant

Department of Mechanical Engineering, University of Utah  
50 S. Central Campus Drive, Rm. 2110, Salt Lake City UT 84112

## ABSTRACT

Microscale electrical field flow fractionation (FFF) has shown significant progress since it was first reported in early 1997. The first electrical FFF systems were lucky to function for more than a few days and generated only minimal levels of retention and separation, while current systems now easily function for years and can generate multicomponent nanoparticle separations. A variety of microscale FFF systems have now been reported including: multiple versions of normal electrical FFF (EIFFF), cyclical electrical FFF (using oscillating fields), dielectrophoretic FFF, thermal FFF, and a combined thermal-electric FFF channel. Related microscale electrical SPLITT systems have also been demonstrated. Microscale EIFFF systems have been used to analyze and separate nanoparticles, DNA, proteins, cells, viruses, liposomes, large polymers, and other materials. EIFFF clearly improves upon system miniaturization due to the reduction in sample and carrier volumes, analysis times and more notably an increase in the separation resolution with a reduction in analysis times. Other advantages of miniaturized FFF include: parallel processing with multiple separation channels, batch fabrication with reduced costs, high quality manufacturing, and potentially disposable systems. Additionally, the possibility of on-chip sample injection, detection and signal processing favors the microfabrication of FFF systems.

Keywords: Microscale field flow fractionation, nanoparticles, microfluidics

## 1. INTRODUCTION

With the recent focus on nanotechnology, the processing of nanoparticles has become increasingly more important and a large research effort has developed to produce uniform nanoparticles. While there are dozens of techniques for producing and sorting nanoparticles, one powerful technique for nanoparticle analysis has shown the widest range of application: field flow fractionation (FFF). Work on miniaturized FFF systems began in the mid 1990's and a wide range of subtypes have been developed, including: normal electrical FFF (EIFFF), cyclical EIFFF, thermal FFF (ThFFF), thermal electric FFF, and others. The related technique, SPLITT, has also been demonstrated on the microscale. The purpose of this work is to review some of the developments in microscale FFF and to examine the capabilities of these systems regarding nanoparticle analysis.

Field-flow fractionation instruments clearly improve when miniaturized due to the reduction in sample and carrier volumes, analysis times and more notably, the increase in the separation resolution (at least for the electrical and thermal subtypes). Other advantages of miniaturized FFF can include: parallel processing with multiple separation channels, batch fabrication with reduced costs, high quality manufacturing, and potentially disposable systems. Additionally, the possibility of on-chip sample injection, detection and signal processing favors the microfabrication of FFF systems. Several demonstrations of the effectiveness of FFF systems on the microscale have been made and will be reviewed in the work.

## 2. BACKGROUND AND THEORY

Field-flow fractionation is a versatile separation technique that relies on the dual effect of the flow behavior and field distribution in a thin, open channel. FFF channels typically consist of a thin spacer enclosed by two parallel plates, modified to impart the external field as shown in Fig.1. Flow in the channel is laminar resulting in a parabolic fluid velocity profile with differential velocity zones across the height of the channel. The versatility of FFF stems from the numerous types of fields and operating modes that can be employed to separate a wide range of sample types. Researchers over the years have developed different types of FFF systems differentiated primarily by the type of the field employed. Electrical, thermal, magnetic, sedimentation, flow and dielectrophoretic fields are all commonly used

---

\* [bruce.gale@utah.edu](mailto:bruce.gale@utah.edu) [www.mems.utah.edu](http://www.mems.utah.edu)

in FFF. In FFF the field is applied perpendicular to the flow of the carrier. Like chromatography, an impulse injection of sample is made into a continuously flowing carrier solution. Under the influence of the applied field, the injected sample migrates to an equilibrium position between the two walls of the channel, as shown in Fig.1. The location of the equilibrium depends on the operating mode of the FFF channel. The average particle in a sample then travels down the channel at the velocity associated with the flow velocity at the equilibrium distance

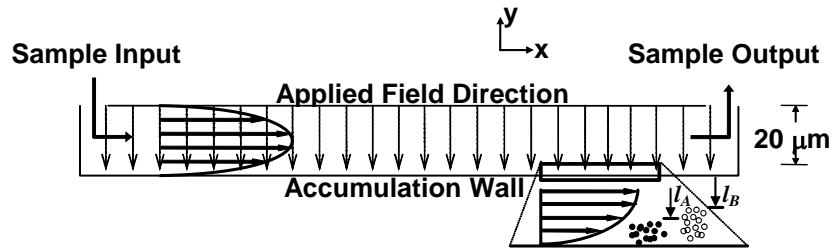


**Fig.1.** Schematic diagram showing FFF operational principle with two parallel plate type channel walls, laminar flow profile with transverse field direction and location of particle clouds near accumulation wall. The particle clouds depicted by closed circles and open circles in inset figure are particle cloud A with average thickness  $l_A$  and particle cloud B with average thickness  $l_B$  respectively.

from the wall. Selectivity in FFF separations is determined by the system's ability to differentially retain the samples based on their physiochemical properties. FFF operational parameters like field and flow rate can be varied to allow the user to tune resolution and analysis times for a given set of sample particles. FFF channels are also naturally gentle and can be used with delicate samples such as cells and liposomes since there is no stationary phase and the shear rates are low. In addition, a single channel can be used to separate a large range of sample sizes, thus enhancing the utility of FFF instruments when compared to many chromatography techniques.

## 2.1. FFF Operating Modes and SPLITT Fractionation

In this work, field-flow fractionation can be classified into three broad modes of operation based on the separation mechanism: (i) normal, (ii) steric, and (iii) cyclical FFF. In normal or classical FFF, the sample particles are forced towards the accumulation wall by the applied field. At the accumulation wall, diffusive forces associated with Brownian motion cause particles to move away from the accumulation wall. At equilibrium, the field induced migrative forces and diffusive forces balance each other and generate an exponential concentration profile of the particle cloud. The average distance  $l$  of the particle cloud from the wall depends on the extent of interaction between the particles and the field and determines the average rate of travel for a particle down the length of the separation channel. For a mixture of particles A and B in a FFF channel as shown in Fig.1, if  $l_A < l_B$ , then the B particles will spend relatively more time in the higher velocity zone and moves faster down the length of the channel compared to the A particles. Thus retention and separation can be generated by manipulating the average distance a particle spends away from the wall. For particles with similar mobilities, larger particles tend to be forced closer to the wall due to their slower diffusion and so smaller particles typically elute from the FFF channel first.

The limit to normal FFF occurs when high field strengths force the sample particles to contact the wall. The distance particles are away from the wall is then controlled by the diameter of the particle or steric effects, and this is referred to as the steric mode of FFF. In steric mode, larger particles protrude farther into the flow stream than do smaller particles and thus larger particles elute first. For microscale systems that generate relatively high fields, the on-set of steric FFF is an important factor in microscale system evaluation. In steric FFF, the elution sequence is reversed in comparison to normal FFF with larger particles eluting earlier.

A recently developed microscale FFF mode involves the use of cyclical fields instead of a steady, uniform field. In this case, particles move either back and forth between the walls or oscillate against one wall of the channel. The retention time for the particle is determined by whether the particle spends more time in the fast flow lines or in the slower flow areas. The amount of time spent in the different flow areas can be tuned by adjusting the field strength and the frequency of the applied field. Cyclical methods have primarily been demonstrated with electrical systems and have the advantage that retention is dependent only upon the susceptibility of the particle to the applied field. Equilibrium processes are not involved and diffusion processes are essentially eliminated from the retention process, so very high speed separations can be generated.

Another technique very closely related to FFF is the split flow thin cell (SPLITT) technique, which generates a continuous separation process. SPLITT has two separate inlets for the sample mixture and a carrier and two outlets for the bifurcated/separated samples. The carrier stream compresses the sample particles against one wall and the field perpendicular to the flow drives sample particles with some minimum interaction across the carrier stream interface where they elute from the opposite outlet. Particles that do not exhibit this minimum interaction with the field continue in the original sample stream and elute from the outlet on the same side as the sample inlet port. SPLITT typically induces very fast fractionation and can be used in serial and parallel fashion to separate complex mixtures with high resolution and high throughput.

## 2.2. FFF Retention Theory

In general, the theory behind FFF systems is well developed<sup>1-3</sup> and in principle the theory can be applied to all the FFF subtypes, including microscale FFF systems. The FFF channel, as shown in Fig.1, is a thin open ribbon like channel of rectangular cross-section with an aspect ratio (the ratio of width to height) over 80 so that channel walls can be closely approximated as two infinite, parallel plates<sup>4,5</sup>. Retention in FFF is the measure of the ability of the system to retain or retard the travel of a particle through the channel compared to a particle unaffected by the applied field. Experimentally, the retention ratio  $R$  is found by

$$R = \frac{t_0}{t_r} = \frac{V_0}{V_e}, \quad (1)$$

where,  $t_0$  is the time required for an unretained particle to exit the channel,  $t_r$  is the time for the retained sample to exit,  $V_0$  is the void volume of the channel and  $V_e$  is the elution volume of the sample. The elution or retention time in FFF is directly related to the properties of the sample and the sample's response to the applied field according to<sup>1</sup>

$$R = 6\lambda \left[ \coth\left(\frac{1}{2\lambda}\right) - 2\lambda \right], \quad (2)$$

where  $\lambda$  is a non-dimensional parameter given by

$$\lambda = \frac{D}{Uw}. \quad (3)$$

where,  $D$  is the particle diffusion coefficient and  $U$  is the field-induced drift velocity, which depends on the applied field strength according to

$$U = \frac{S'\phi}{f'}, \quad (4)$$

where,  $S'$  is the applied field strength,  $\phi$  is the field susceptibility of the particles and  $f'$  is the sample friction coefficient. Note that the form of equation 4 will vary somewhat depending on the type of field used in the particular FFF system. The diffusivity,  $D$ , for a nanoparticle can be calculated using the modified Einstein equation

$$D = \frac{\kappa T}{3\pi\eta d}, \quad (5)$$

where,  $\kappa$  is Boltzmann's constant,  $T$  is the absolute temperature, and  $d$  is the particle diameter.

## 3. MICROSCALE ELECTRICAL FIELD-FLOW FRACTIONATION

Electrical field-flow fractionation was the first FFF subtype to be miniaturized using MEMS techniques<sup>6</sup>. In EIFFF, a voltage is applied across the two channel walls bounding the FFF channel<sup>7</sup>. The separation criteria is based on the  $\zeta$ -potential or electrophoretic mobility possessed by the particles suspended in the carrier solution, which is typically DI

water or a low ionic strength buffer. With the ability to measure the electrophoretic mobility of sample particles with known sizes, EIFFF can be used both as a separation unit or a diagnostic instrument.

Applications of EIFFF include: separation of cells and organelles, bacteria and viral separations, characterization of emulsions, liposomes and other particulate biological vehicles, separation of macromolecules, environmental monitoring, and biomaterial studies. EIFFF has been used to study protein adsorption by analyzing surface modified particles for biomaterial applications. In addition to many of these applications, Gale et al. have employed  $\mu$ -EIFFF in whole blood separations for medical diagnostics<sup>8</sup>. EIFFF also finds application as a sample pretreatment system by performing an initial separation on a sample that can later be collected for further testing by another analysis system. For example, EIFFF can be used as a sample preparation unit prior to a PCR step in a total analysis system.

A major advantage EIFFF enjoys over similar separation systems is low power and voltage requirements. In comparison to electrophoresis systems which typically require several thousand volts, EIFFF operates below 3 V. Even such a small amount of applied voltage across thin EIFFF channel results in a voltage gradient similar to that in electrophoresis systems that operate at about 1000 times higher voltage. Thus, miniaturization proves beneficial in reducing power requirements and raises the possibility of a portable instrument with small batteries as power source.

### 3.1. Theory

Most of the general FFF equations can be applied directly to EIFFF by replacing  $U$  in the particular equation. For example,  $\lambda$ , the non-dimensional parameter relating experimental parameters to  $R$ , is represented by

$$\lambda = \frac{D}{\mu E w} = \frac{\kappa T}{3\pi\eta\mu E w}, \quad (6)$$

where,  $\mu$  is the electrophoretic mobility of the sample and product of  $E$  and  $w$  is effective voltage  $V_{eff}$ . Equation 6 shows that retention in EIFFF systems is still inversely proportional to  $w$ , but since the effective field  $E$  is also a function of channel height, there is no effect on retention as the channel is miniaturized. While this conclusion may seem to indicate that there is no net benefit in terms of retention from miniaturization, the fact that there is no disadvantage allows for the system as a whole to derive a significant advantage from miniaturization.

The mechanics of EIFFF are different from most other FFF systems due to the presence of the electrical field and its interaction with the aqueous carrier. An electrical double layer is created at the interface of the polarized electrode and carrier solution. A major portion of the applied field drops across this double layer resulting in an effective field in the bulk of the channel that is only a fraction of the applied voltage available for retention of the sample. Effective voltages on the order of 1% have been reported in case of  $\mu$ -EIFFF systems<sup>9,10</sup>. This loss of effective field is caused by two related electrochemical phenomena. First, a significant portion of the voltage drops at the electrode / carrier interface which may be attributed primarily to the electrode material properties. Second, the applied voltage has to overcome a potential barrier before any significant charge-transfer starts between the electrode and the carrier solution. The severity of the effective field reduction depends largely on the thickness of the double layer or the ionic strength of the carrier solution. A compact double layer, as occurs with a high ionic strength carrier, may result in very low field in the bulk with little or no retention in the channel. A critical concern regarding miniaturization of EIFFF is the creation of a more compact double layer and relatively low ionic strength solutions that can be used in the systems.

If the effective field is very low, the first solution to solving the problem would be to raise the applied voltage. Unfortunately, since the electrodes are in direct contact with an aqueous carrier, at voltages over about 2 V, electrolysis occurs and bubbles are rapidly generated that destroy the flow profile and cause severe mixing that makes the system nonfunctional. Thus, applied voltages are generally proscribed to a value where electrolysis does not occur.

One of the major challenges in EIFFF is the determination of the effective field and its associated retention of sample in the EIFFF channel. Unfortunately, this problem is highly complex and involves a number of operational and instrument variables such as voltage, sample, carrier composition, pH and ionic strength, electrode material and history, and so on. Only a rudimentary model for simulating transport properties using the convection-diffusion equation has been presented by Chen et al.<sup>11</sup>. The convection-diffusion equation was used to mimic ion and particle transport (DNA with an anisotropic diffusion coefficient) in EIFFF with an arbitrary value for the effective field (0.5% of applied voltage). The standard theory of EIFFF, though, embeds the solution to the convection-diffusion equation as illustrated by Palkar

et al.<sup>12</sup> and numerical solution is not generally required if an effective field value is assumed, even for a sample with anisotropic diffusion. A more complete understanding of the inner workings of an EIFFF channel has not yet been presented, though empirical models have been presented by Kantak et al.<sup>10,13</sup>.

### 3.2. Fabrication and Packaging

Semiconductor fabrication processes were applied towards fabrication of the earliest  $\mu$ -EIFFF systems as outlined in Fig. 2<sup>6</sup>. KOH etching was used to realize input and output ports on a silicon wafer. Titanium and gold layers were sputtered on the silicon as well as a glass substrate used as the second wall of the FFF channel. Platinum has also been used as an electrode material<sup>10</sup>. Thick photosensitive polyimide/SU-8 was photolithographically patterned to realize the microfluidic channels and provide a spacer between the electrodes. In several versions of the system, an adhesive trough was provided around the channel to facilitate adhesive bonding of the silicon wafer with polymer channel to a glass substrate with identical channel electrodes. For fluidic connections, PEEK tubing was attached to the silicon wafer over the ports using a ferrule glued to the substrate. Electrical connections were made by bonding wires to extensions of the electrodes. Another microfabricated system was reported by Lao et al. that used indium tin oxide (ITO) as electrodes<sup>14</sup>. ITO (transparent ceramic) coated glass of 3 mm thickness was patterned to obtain electrodes with sheet resistance of 14  $\Omega$ /cm. This manufacturing process also used SU-8 as channel walls.

For more recent microscale EIFFF systems, the fabrication process was modified so as not to include any special micromachining processes and yet still achieve the advantages related to the miniaturized systems. In this design, polished graphite plates were used as both channel electrodes and a microfluidic channel was cut in a 25  $\mu$ m thick double side adhesive tape, using xurography, an inexpensive rapid prototyping tool based on knife plotting<sup>15,16</sup>. This system provided more reproducible fabrication results in a cost effective manner and proved efficient in producing prototypes for research purposes.

Typical  $\mu$ -EIFFF system geometrical dimensions are 6 cm length, 2 mm width and 25  $\mu$ m height in comparison to a macroscale channel of 64 cm length, 2 cm width and 176  $\mu$ m height. The sample injection for microsystem is reduced to 0.1  $\mu$ L from a 1-5  $\mu$ L for macroscale system.

### 3.3. Retention

Retention is directly related to current in EIFFF and a plot of the inverse of current with retention ratio  $\lambda$ , shows that retention in microscale systems follows the theoretical predictions and that a straight line through the data goes through the origin as shown in Fig. 3a<sup>10</sup>. Microscale EIFFF systems have been demonstrated for a range of samples, conditions, and configurations. An example of differential retention of particles based on a difference in electrophoretic mobility is shown in Fig. 3b.

A retention related EIFFF characteristic is size selectivity, which is a measure of a systems ability to separate based on size. Typically, macrosystems possess size selectivity between 0.67 to 1<sup>7</sup>, but size selectivity in microscale EIFFF has been shown to be close to unity<sup>10</sup>.

### 3.4. Separations

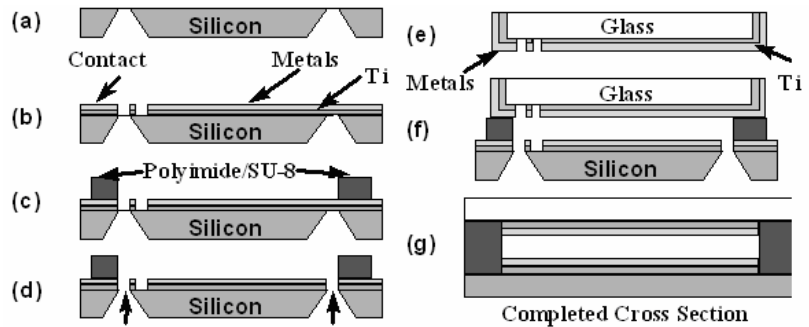


**Fig. 2.** Fabrication flow chart for the  $\mu$ -EIFFF system. (a) Etching of input and output ports in silicon. (b) Deposition and patterning of titanium as adhesion layer and gold as channel electrode. (c) Spinning and patterning of polyimide/SU-8 as channel walls. (d) Removal of Si<sub>3</sub>N<sub>4</sub> membranes. (e) Deposition and patterning of titanium as adhesion layer and gold as channel electrode on glass. (f) Bonding of glass and silicon substrate using UV-curable adhesive. (g) Cross-section of completed  $\mu$ -EIFFF system.

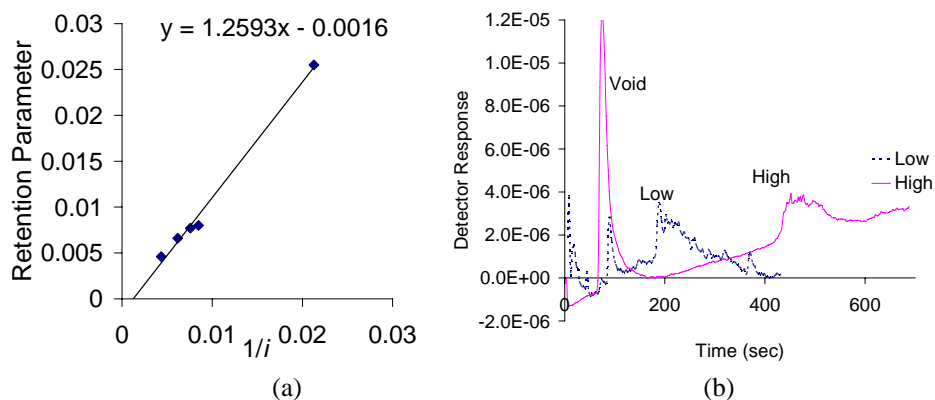


**Fig. 3.** Retention results in EIFFF<sup>10</sup>. **(a)** Graph of retention parameter,  $\lambda$ , compared to the inverse of the measured current,  $1/i$ . The experiments were performed using 94 nm PS particles in DI water with a flow rate of 0.3 mL/hour in a system with platinum electrodes. **(b)** Fractograms of particles with the same diameter, but differing levels of carboxylation. The run labeled “low” had a lower density of COOH groups on the surface (67  $\mu\text{eq/g}$ ) compared to the sample labeled “high” (510  $\mu\text{eq/g}$ ). The carrier was DI water with a voltage of 1.392 V (10  $\mu\text{A}$ ) and a flow velocity of 1.48 mm/s. Reprinted with permission from<sup>10</sup>. Copyright (2002) American Chemical Society.

A goal for  $\mu$ -EIFFF is high-speed separations that can be detected using an on-chip detector<sup>10</sup>, which should significantly reduce band broadening and maximize resolution. Fig. 4a shows such a separation of a multicomponent polystyrene particle mixture in under 120 s. A separation of identical resolution in a macroscale system would require 2 h. As shown in Fig. 3b  $\mu$ -EIFFF can also generate charge based separation, an attractive feature for biological separations. Fig. 4b demonstrates how identical particles with and without proteins attached to the surface can be differentially retained and separated in a  $\mu$ -EIFFF system. Separations of blood components both before and after homogenization have been demonstrated using these same systems<sup>8</sup>.

The retention and separation data for  $\mu$ -EIFFF was obtained with an on-chip conductivity detector<sup>18,19</sup>. The on-chip conductivity detector was used to minimize the band broadening due to post-column volumes and to maximize the miniaturization related advantages of the  $\mu$ -EIFFF channel. Another type of on-chip detection scheme employed with  $\mu$ -EIFFF was based on the resonance light scattering (RLS) principle<sup>20</sup>. On-chip RLS is based on the shift in absorption and scattering spectral profiles for different particles i.e. different sized particles yield different colored scattered light. The main advantages of this technique include: its noninvasive nature, high sensitivity for particle detection, and low cost.

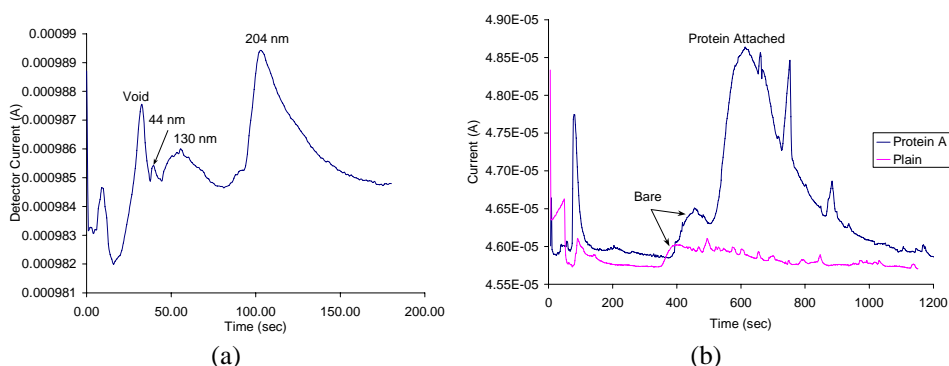


**Fig. 4.** Separations performed in microscale EIFFF system. **(a)** Separation of a mixture of polystyrene particles detected using an on-chip conductivity detector. The operating conditions are 1.6 V, 0.3 ml/h flowrate and 27  $\mu\text{A}$  current in a 2 mm wide channel with platinum electrode with DI water carrier. Reprinted with permission from<sup>10</sup>. Copyright (2002) American Chemical Society. **(b)** Fractograms showing differential retention and separation between bare particles and particles with attached protein A<sup>17</sup>.

### 3.5. Effective Field Scaling

The most important performance factor in EIFFF is the effective field. Since the effective field in the channel is difficult to determine using transport and electrochemical models, the effective field is usually calculated from retention data of standardized particles with known electrophoretic mobility. The effective electric field,  $E_{eff}$ , responsible for the given retention is then calculated using

$$E_{eff} = \frac{6Dt_r}{\mu w t_0} = \frac{2\kappa T t_r}{\mu w \pi \eta d t_0} \quad (7)$$

The effective field calculated using equation 7 is generally only ~1% of the applied field. Fig. 5 shows the measured effective field for a  $\mu$ -EIFFF system as a function of current density and shows that microscale systems significantly outperform macroscale systems, which are constrained to the boxes drawn in each figure. It can be seen that macroscale system is more efficient in terms of generating more effective field in comparison to microscale system for a given amount of current, but the amount of effective field that can be generated using a microsystem far exceeds that of a macroscale system. The limits in this comparison may be related to the electrode composition (platinum for microscale, graphite for macroscale) and similar data generated for graphite microsystems may show even better results.

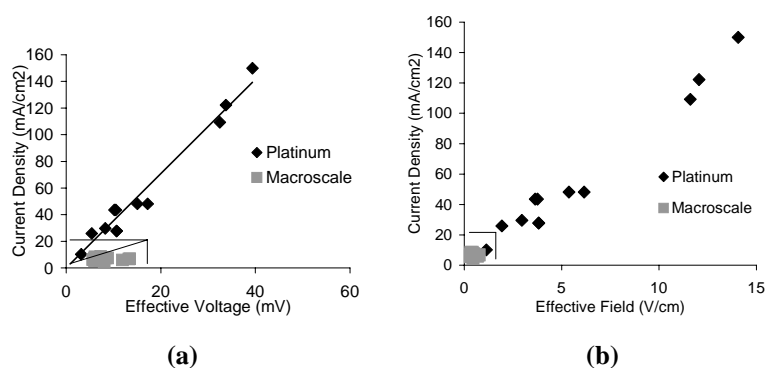


**Fig. 5.** Comparison of electrical properties of microscale and macroscale EIFFF system. The boxes in both figures represent the limits of the macroscale system. Plots show (a) effective voltage and (b) effective field as a function of current density for both systems. Platinum refers to data from a platinum-based microscale system. Reprinted with permission from<sup>10</sup>. Copyright (2002) American Chemical Society.

## 4. MICROSCALE CYCLICAL ELECTRICAL FIELD-FLOW FRACTIONATION

Once  $\mu$ -EIFFF channels had been developed, efforts were made to determine methods to overcome the electrochemical limits associated with EIFFF. Cyclical fields were proposed as a way to overcome some of the capacitance associated with the double layer and drive effective fields up substantially. This method has proven very effective and has turned into a useful method worth considering on its own. Note that Cyclical Field-Flow Fractionation (CyFFF) was first proposed as a method by Giddings in 1986<sup>21</sup> and demonstrated using a gravitational FFF system<sup>22</sup>, but the only microscale systems have been electrical (CyEIFFF). Thus, CyEIFFF will be the focus of this text, though much of the analysis also applies to other CyFFF techniques.

Physically, a CyEIFFF system is identical to an EIFFF system and both techniques can be performed using the same channel and electrode setup<sup>23,24</sup>. As shown in Fig. 6, the mechanics of CyFFF are quite different from normal FFF due to the presence of the oscillating field.

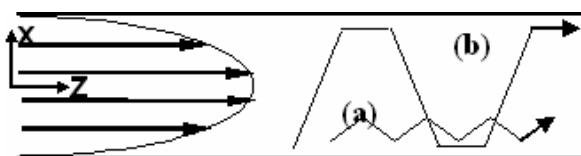


**Fig. 6.** Schematic diagram of the particle mechanics for (a) CyFFF mode I and (b) CyFFF mode III.

Unlike normal EIFFF, the particles interacting with the field do not reside near the accumulation wall or form a static exponential concentration profile (Fig. 6a) but move back and forth between the parallel electrodes under the influence of cyclical field. A number of operational and physical parameters (applied voltage and its frequency, electrophoretic mobility and size of the particles, flow rate, pH and ionic strength of the carrier solution) determine how fast and how far the sample particles move between the electrodes and the average location of the particles in the channel. Depending on the motion of the particles, a particular group of particles will spend more or less time in the faster

velocity zone (away from the channel electrodes) compared to other particles, generating differential retention and separation.

Based on the magnitude of the particle movement between the channel electrodes, CyEIFFF can be classified into three different modes of operation. If particles oscillate only against one wall/ electrode and do not completely cross the channel and reach the other wall, the particles are operating in Mode I. If the particles completely cross in one half cycle and rest for some period against the opposite wall, the particles are operating in mode III. Mode II occurs when particles reach the opposite wall just as the field is reversed.

#### 4.1. Theory

In CyEIFFF the retention ratio, R can be related to a non-dimensional parameter  $\lambda_0$ , which for an applied square wave electrical field is given by

$$\lambda_0 = \frac{\mu E_{eff}}{2fw} = C \frac{\mu E_{eff}}{fw^2}, \quad (8)$$

where, f is the frequency of the field oscillation in Hz.  $\lambda_0$  values can be used to determine the mode of CyEIFFF operation and retention ratio R. For mode I, R is given by

$$R = 3\lambda_0 \left(1 - \frac{2\lambda_0}{3}\right) \text{ for } \lambda_0 \leq 1; \quad (9)$$

whereas, for Mode III R is given by

$$R = \frac{1}{\lambda_0} \text{ for } \lambda_0 \geq 1. \quad (10)$$

Mode II can be represented by either model as the unity value of  $\lambda_0$  holds true for both equations 9 and 10.

#### 4.2. Experimental Results

CyEIFFF has shown the ability to significantly retain nanoparticles and to perform separations on nanoparticles, especially using low ionic strength carriers. Examples of some of these experiments are summarized in the following sections.

Fig. 8 shows the typical elution characteristics of the  $\mu$ -CyEIFFF as a function of frequency of the applied field<sup>13</sup>. It can be deduced from Fig. 8 that Giddings's model clearly does not match with the experimental data and deviates even with the inclusion of steric and diffusion effects. Elution times computed using the estimated effective field instead of the nominal field yield a better match with the experimental results and show that electrical double layer related effects are of prime importance in CyEIFFF. Also, mode transition can be predicted correctly with the use of the lumped electrical parameter model for the evaluation of  $\lambda_0$ .

Lao et al. showed that the increased effective field with the pulsed field resulted in 50 fold increase in current and that there was a strong influence of pulse frequency on retention time<sup>14</sup>. The retention dependence on voltage is straightforward and an increase in applied voltage results in increased retention when in Mode III. For example, the elution time quadruples when the peak to peak voltage (square wave at 1 Hz) is increased from 1 V to 8 V for retention of 100 nm

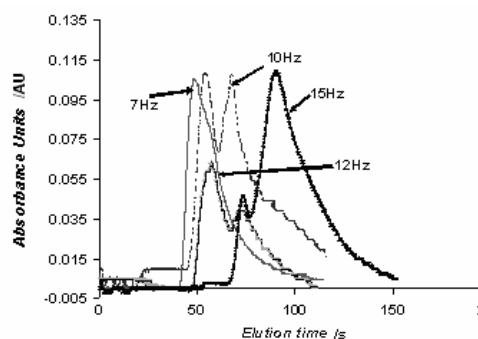


**Fig. 7.** Separations of 100 nm silica nanoparticles (first peak) and polystyrene (PS) amine group nanoparticles (second peak). The operating conditions are a square wave of 3.0 VPP with 0.3 VDC offset, 1.0 mL hr<sup>-1</sup> flow rate (DI water of pH 7.4±0.1).<sup>24</sup> -Reproduced by permission of The Royal Society of Chemistry.

amino coated polystyrene nanoparticles in a 50  $\mu\text{M}$  ammonium carbonate carrier.

### 4.3. Separations

Separations in  $\mu\text{-CyEIFFF}$  are dependent on a difference in the electrophoretic mobility of the samples. In the earliest separation results published by Lao et al., pulsed EIFFF was able to resolve a separation of 0.105  $\mu\text{m}$  and 0.405  $\mu\text{m}$  particles<sup>14</sup>.

Fig. 7 shows high-speed separations (<3 minutes) of nanoparticles using  $\mu\text{-CyEIFFF}$ <sup>24</sup>. It can be seen that resolution is highly dependent on frequency and in this case separation resolution increases with the frequency of the applied field. It should be noted that plate heights also vary with frequency and tend to follow a pattern similar to the elution times (Fig. 8) with a minimum plate height obtained near the mode transition point. This translates to limits on separation power in  $\mu\text{-CyEIFFF}$  with reduced peak capacities in comparison to  $\mu\text{-EIFFF}$ . An offset voltage is used to force the particles towards one accumulation wall while operating in mode I to relax the sample and avoid initial random distribution of the particles across the channel height.

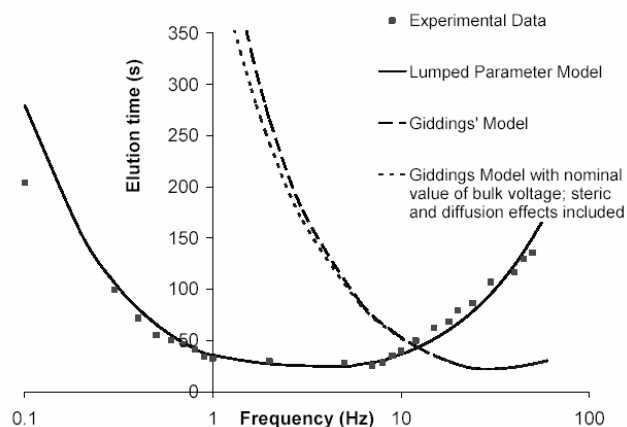


**Fig. 8.** Comparison between model and experimental model for  $\mu\text{-CyEIFFF}$  system. Reprinted with permission from <sup>13</sup>. Copyright (2006) Wiley.

## 5. MICROSCALE THERMAL FIELD-FLOW FRACTIONATION

Thermal field-flow fractionation (ThFFF), one of the oldest FFF subtypes, has primary application in the separation and analysis of dissolved and suspended polymer samples. ThFFF utilizes a temperature gradient across the channel walls to induce separation based on a particle's thermal diffusion coefficient. ThFFF is similar to EIFFF in that the gradient of temperature generates the field, just as the gradient of voltage generates retention in electrical FFF. To generate the temperature gradient, thermally conductive channel walls are maintained at different temperatures. Polymers typically migrate towards the cold wall and the balance between transport and diffusion determines particle retention. A range of solvents such as methanol, THF, acetonitrile, DMSO, toluene and aqueous solutions with different types of detergents have been employed as carriers in ThFFF.

Applications of ThFFF include: molecular weight and size distribution determination, particle size measurement, thermal diffusion coefficient measurements, physicochemical and surface property studies and separation of particle colloidal mixtures.

Retention in ThFFF system depends on the Soret coefficient, a ratio of thermal diffusion and Fickian diffusion coefficients. The retention parameter can be related to these sample physicochemical properties by

$$\lambda = \frac{D}{(D_T \Delta T)} = \frac{\kappa T}{3\pi\eta} \left[ \frac{10\pi N_A}{3[\eta]MW} \right]^{1/3} \frac{1}{(D_T \Delta T)}, \quad (11)$$

where,  $D_T$  is the thermal diffusion coefficient,  $\Delta T$  is the temperature drop across the channel height,  $\kappa$  is the Boltzmann's constant,  $T$  is the average temperature,  $\eta$  is the average carrier viscosity,  $N_A$  is the Avogadro's constant,  $[\eta]$  is the intrinsic viscosity of the dissolved sample, and MW is the average molecular weight of a dissolved sample.

The first successful microfabricated ThFFF system was demonstrated by Edwards et al.<sup>25</sup> and was followed by several reports on mesoscale ThFFF with reduced geometrical dimensions<sup>26,27</sup> and a microfabricated ThFFF without showing any particle separation<sup>28</sup>. The early ThFFF microsystems were fabricated using techniques similar to the  $\mu\text{-EIFFF}$  fabrication (Fig. 2) with a 27  $\mu\text{m}$  channel thickness, 2-4 mm breadth and 4-6 cm length. These microsystems made of silicon and glass with SU-8 to define the channel walls were fabricated using conventional microfabrication techniques. A thin-film titanium heater on silicon or boron-doped silicon heaters were used to generate the hot wall whereas a glass

slide was used as the cold/accumulation wall. Results obtained this early microsystem presented showed a poor temperature drop across the channel due to a poor heat transfer setup. Essentially, silicon with its very high thermal conductivity was found to waste a lot of input energy that was transferred to the environment rather than across the channel. In addition, glass has a high heat capacity and acts as an insulator making it difficult to maintain a good cold wall temperature. The overall result of these efforts was a very low effective temperature drop available for retention and separation. Later communications<sup>29</sup> from our group showed how the efficiency of heat transfer in ThFFF can be improved by just switching the roles of silicon and glass to cold wall and hot wall respectively. Even with a low temperature drop of  $\sim 5.3^{\circ}\text{C}$ , retention ratios of 0.46 and 0.33 for particles of 204 nm and 272 nm were obtained in a clear separation. Power consumption was reduced 300 fold for a one order of magnitude smaller temperature drop generating similar results when compared to a macroscale system.

## 6. OTHER MICROSCALE FIELD-FLOW FRACTIONATION EFFORTS

A few other non-conventional FFF techniques have been developed at the microscale, but only a little information has been published on them. For example, the FFF-like SPLITT system, zero-field hydrodynamic chromatography, and a dual field thermal-electrical FFF system have been demonstrated on the microscale. These techniques hold a lot of promise as they expand the FFF applications and provide researchers with more versatile instrumentation.

A microfabricated thermal-electrical system that is capable of imparting both thermal and electrical fields simultaneously using a single instrument was demonstrated on nanoparticles. This system improved retention by 20% with the use of a thermal field ( $15^{\circ}\text{C}$  temperature difference) in conjunction with the electrical field<sup>29</sup>. This device design also demonstrated better channel wall material selection can increase the temperature drop across the  $\mu$ -ThFFF channel

A technique for minimizing end effects in FFF channels was uniquely demonstrated in a microscale FFF system<sup>30</sup>. For this work, microstructures in the triangular inlet end-pieces were used to distribute sample uniformly across the breadth of the microchannel. A comprehensive fluid flow analysis was used to optimize the size, shape and locations of the microstructures. Particle dispersion analysis and experimental plate height measurements showed close to a 50% reduction in total plate height for common FFF operating conditions.

### 6.1. Microscale Split-Flow Thin Fractionation

Split flow thin fractionation (SPLITT) cell is a separation technique very similar to FFF in principle and geometry<sup>31</sup>. Unlike FFF, SPLITT operates continuously and separates the sample stream into two fractions. Since SPLITT can operate continuously, it is ideal for use in applications where high throughput is required.

SPLITT channels have two inlets to introduce the sample and carrier solutions respectively, and two outlets to elute the separated fractions as shown in Fig. 9. The inlet flow splitter prevents unwanted mixing of the two inlet streams and forces the sample input line into a thin stream along one wall of the channel and thus forming the inlet splitting plane (ISP). The applied field perpendicular to the flow of the solution forces susceptible particles across the ISP towards the opposite wall, inducing a binary separation based on the particles' susceptibility to the applied field. The system in Fig. 9 is an example of transport mode SPLITT where the higher transport rates of the black particles allows them to cross the ISP and elute through the lower outlet. For those familiar with microfluidics, this system is similar to the H-filter in principle<sup>32</sup>, but adds an external field instead of a concentration gradient as the driving force, which gives SPLITT the possibility of high power separations with higher resolution.

The inherent capability of the system to divide a sample based on a property of the sample particles provides the impetus for sequential or serial separation to yield high volume separation of a complex multicomponent sample. As a first step towards achieving this goal, a microfabricated electrical SPLITT system

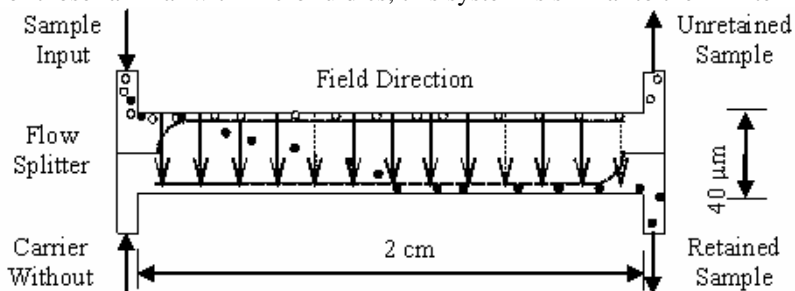


**Fig. 9.** Schematic diagram of SPLITT system with input and output connections for sample and carrier flow with field direction and illustration of the separation mechanism.

was fabricated and characterized using polystyrene nanoparticles<sup>31</sup>. Micromachining techniques were used to fabricate a 40  $\mu\text{m}$  thick (channel height) and 2 cm long channel on a glass substrate with gold electrodes in a method similar to that for  $\mu\text{-EIFFF}$ . The microchannel was realized using SU-8 and bonded to another glass substrate using UV curable adhesive.

Characterization of the system was done using a mixture of 108 nm ( $\mu$  of  $2.47 \times 10^{-4} \text{ cm}^2 \text{V}^{-1} \text{s}^{-1}$ ) and 220 nm ( $\mu$  of  $4.48 \times 10^{-4} \text{ cm}^2 \text{V}^{-1} \text{s}^{-1}$ ) diameter polystyrene particles with amine surface groups. SEM images of the eluted particles showed 94% 220 nm particles in one outlet and 70% 108 nm particles in other outlet, a high number selectivity separation at only 1.2 V across the channel. A logical solution to improve the resolution of 108 nm particle sample would be to pass it through another SPLITT channel and adjust the voltage to further separate out 220 nm particles from this stream.

The microfabricated electrical SPLITT system showed potential as a powerful separation technique even with only a 1% effective field due to double layer effects. Serial and parallel combinations of SPLITT channels should result in high resolution and high throughput separations of nanoparticles. In electrical SPLITT system it is relatively easy to control the electrical field in designated areas when compared to thermal or magnetic systems. The ability to program each electrical SPLITT channel separately should result in a tunable resolution and should increase the robustness of the system. There is still significant room for determining optimized channel dimensions for a variety of sample sizes and types in microscale electrical SPLITT channels.

## 7. CONCLUSION

Microscale FFF has shown significant progress since it was first published in early 1997<sup>33</sup>. Various microscale FFF systems have been used to analyze nanoparticles, DNA, proteins, cells, viruses, polymers, and other materials. A summary of applications are provided in Table 1. Several research groups are now actively exploring applications for these technologies. Since many formats of FFF show significant scaling advantages, there is an opportunity for improvement in these technologies as they are miniaturized. With the advent of the first nanoscale systems, the final potential of these systems is just becoming evident. These FFF channels have also been integrated into more complex analysis systems, and have the potential to be integral components of a lab-on-a-chip system because of their simple operation and easy tuning for specific applications. There are also opportunities to investigate subtechniques in microscale FFF such as magnetic, flow, or sedimentation FFF, which have not yet been explored. Overall, significant promise has been shown, but substantial work needs to be completed before these techniques will be applied broadly.

**Table 1.** Summary table for microscale field-flow fractionation systems

FFF Subtype	Physiochemical Properties	Applications
Electrical	Size, electrophoretic mobility	Cells and organelles, bacteria and viral separations, characterization of emulsions, liposomes, protein adsorption
Thermal	Size, thermal diffusion coefficient	Separation of dissolved and suspended polymers, polymer and silica nanoparticle analysis
Cyclical Electrical	Electrophoretic mobility	Biopolymer separations and zeta potential measurements
Dielectrophoresis	Dielectric permittivity, size	Cell Separation and dielectric property measurements and cancer cell separation
Electrical SPLITT	Size, electrophoretic mobility	High-throughput nanoparticle purification, proteins and starch, clay, viruses, spores, bacteria
Asymmetrical Flow	Density, size	Proteins, DNA, polymers, cells, micro and nanoparticles
Hydrodynamic Chromatography	Size	Large macromolecule without any charge requirement
Acoustic	Size, density or compressibility	Macromolecules and nanoparticles

## 8. ACKNOWLEDGEMENTS

The authors acknowledge funding from the State of Utah Center of Excellence program for some of this work.

## 9. REFERENCES:

1. Giddings J (1968) Non-equilibrium theory of field-flow fractionation *J. Chem. Phys.* 81-85:49
2. Giddings J, Caldwell K (1989) Field-flow fractionation. In Rossiter B, Hamilton J (eds) *Physical Methods of Chemistry Vol IIIB*. John Wiley and Sons, New York
3. Schimpf M (2000) Resolution and fractionating power In Schimpf M, Caldwell K, Giddings J (eds) *Field-flow fractionation handbook*. Wiley-Interscience, New York, pp 71-79
4. Giddings J, Schure M, (1987) Theoretical analysis of edge effects in field-flow fractionation. *Chem. Eng. Sci.* 42: 1471-1479
5. Hovingh M, Thompson G, Giddings J, (1970) Column parameters in thermal field-flow fractionation. *Anal Chem* 42: 195-203
6. Gale B, Caldwell K, Frazier A (1998) A micromachined electrical field-flow fractionation ( $\mu$ -EFFF) system. *IEEE Tran. Biomed. Engg.* 45:1459-1469
7. Caldwell K, Gao Y (1993) Electrical field-flow fractionation in particle separation. 1. monodisperse standards. *Anal Chem* 65: 1784-1772
8. Gale B, Caldwell K, Frazier A, (2000) Blood and protein separations using a micromachined electrical field-flow fractionation system *Proc. of MicroTAS 2000*, Enschede, Netherlands pp 399-402
9. Gale B, Caldwell K, Frazier A (2001) Geometric scaling effects in electrical field-flow fractionation. 1. theoretical analysis. *Anal Chem* 73: 2345-2352
10. Gale B, Caldwell K, Frazier A (2002) Geometric scaling effects in electrical field-flow fractionation. 2. experimental results. *Anal Chem* 74: 1024-1030
11. Chen Z, Chauhan A (2005) DNA separations by EFFF in a microchannel. *J. of Co. and Int. Sci.* 285: 834-844
12. Palkar S, Schure M (1997) Mechanistic study of electrical field-flow fractionation. II: The effect of sample conductivity on retention. *Anal Chem* 3230-3238
13. Kantak A, Merugu S, Gale B (2006) Particle size and electric field effects in cyclical electrical field-flow fractionation. *Electrophoresis* 27:2833-2843
14. Lao A, Trau D, Hsing I (2002) Miniaturized flow fractionation device assisted by a pulsed electric field for nanoparticle separation. *Anal Chem* 74: 5364-5369
15. Sant H, Gale B (2004) Flexible coupling of a waveguide detector with a microscale field-flow fractionation device. *Proc. of SPIE* 5345:250-257
16. Bartholomeusz D, Boutte R, Andrade J (2005) Xurography: rapid prototyping of microstructures using a cutting plotter. *JMEMS* 14: 1364-1374
17. Gale B, Scaling effects in a microfabricated electrical field-flow fractionation system with integrated detector, Ph.D. dissertation, University of Utah, September 1999
18. Gale B, Caldwell K, Frazier A, (1998) Electrical conductivity particle detector for use in biological and chemical micro-analysis systems. *Proc. SPIE* 3515: 230-242
19. Gale B, Frazier A, (1999) Electrical impedance spectroscopy particle detector for use in microanalysis systems. *Proc. SPIE* 3877: 190-201
20. Graff M, Frazier A, (2006) Resonance light scattering (RLS) detection of nanoparticle separations in a microelectrical field-flow fractionation system. *IEEE transactions on nanotechnology* 5:8-13
21. Giddings, J.C. (1986) Cyclical field flow fractionation: A new method based on transport rates. *Anal Chem* 58: 2052-2056
22. Lee S, Myers M, Beckett R, Giddings J, (1988) Experimental observation of steric transition phenomena in sedimentation field-flow fractionation *Anal Chem* 60: 1129-1135
23. Gale B, Merugu S (2005) Cyclical electrical field flow fractionation. *Electrophoresis* 26:1623-1632
24. Kantak A, Merugu S, Gale B, (2006) Characterization of a microscale cyclical electrical field flow fractionation system. *Lab Chip* 6: 645 - 654
25. Edwards T, Gale B, Frazier A (2002) *Anal Chem* 74:1211-1216
26. Janca J (2002) Micro-channel thermal field-flow fractionation: new challenges in analysis of macromolecules and particles. *J. Liq. Chrom. & Rel. Technol.* 25: 683-704
27. Janca J, Ananieva I, Menshikova A, Evseeva T, Dupak J (2004) Effect of channel width on the retention of colloidal particles in polarization, steric, and focussing micro-thermal field-flow fractionation. *J. of Chromatogr. A* 1046:167-173
28. Bargiel S, Dziuban J, Gorecka-Drzazga A (2004) A micromachined system for the separation of molecules using thermal field-flow fractionation method. *Sens. & Act. A* 110:328-335
29. Sant H, Gale B (1991) A microfabricated thermal electric field flow fractionation system. in *Proc. of MicroTAS 2001*, pp 563-564
30. Sant H, Kim J, Gale B (2006) Reduction of end-effect induced zone broadening in field-flow fractionation channels, *Anal Chem* in press
31. Narayanan N, Saldanha A, Gale B (2005) A microfabricated electrical SPLITT system *Lab Chip* 6:105-114
32. Brody J, Yager P (1997) Diffusion-based extraction in a microfabricated device. *Sensors and Actuators A: Physical*, 58: 13-18
33. Gale B, Frazier A, Caldwell K (1997) A micromachined electrical field- flow fractionation system, in *Proc. 10th IEEE International Workshop on Micro Electro Mechanical Systems (MEMS '97)*, Nagoya, Japan, Jan. 26-30, pp. 317-322